Materials Science-Poland, Vol. 25, No. 2, 2007

Mössbauer investigations of the magnetic structure of γ-Fe–Mn

K. SZYMAŃSKI[1*], W. OLSZEWSKI[1], D. SATUŁA[1], L. DOBRZYŃSKI[1, 2]

[1]Institute of Experimental Physics, University of Białystok, 15-424 Białystok, Poland

[2]The Sołtan Institute for Nuclear Studies, 05-400 Otwock-Świerk, Poland

Mössbauer polarimetry was used for investigations of orientations of Fe magnetic moments in a γ-Fe–Mn system. External magnetic field was applied to single crystal samples. Since the hyperfine field is a vector quantity, it forms a vector sum with the external magnetic field, and this quantity obviously depends on the magnetic structure of a system under study. Investigations with various orientations of external magnetic field with respect to the crystalline directions were performed. There is a clear experimental evidence that the distribution of Fe moments is present, which explains the already reported disagreement between simulated and measured results. Shapes of the spectra are best explained under the assumption of a coexistence of Q_2 and Q_3 structures. Influence of plastic deformation on the distribution of hyperfine fields is reported.

Key words: *γ-Mn-Fe alloy; manganese alloy; iron alloy; plastic deformation; Mössbauer spectroscopy*

1. Introduction

Magnetic structure of chemically disordered alloys in which atoms occupy *fcc* lattice positions has been a subject of intensive investigations. The symmetry of cubic structure allows at least three various antiferromagnetic structures with wave vectors $Q_1 = (1,0,0)$, $Q_2 = (1,1,0)$ and $Q_3 = (1,1,1)$, respectively. Because of formation of antiferromagnetic domains, all the magnetic structures result in the same neutron diffraction pattern. This makes experimental discrimination between the structures very difficult.

Mössbauer spectroscopy is sensitive to the direction of hyperfine magnetic field. Hyperfine magnetic field is a vector sum of external magnetic field and the local field. Thus the distribution of hyperfine fields observed in Mössbauer experiments depends on the magnetic structure (Q_1, Q_2 or Q_3) and the external magnetic field. The first measurements of single crystal γ-$Mn_{44.2}Fe_{55.8}$ by Kennedy and Hicks [1] disproved the

*Corresponding author, e-mail: kszym@alpha.uwb.edu.pl

Q_1 structure. Neither was the agreement of the spectra measured in the fields up to 9 T with simplest predictions for Q_2 or Q_3 structures satisfactory.

Other experiments were performed on $Mn_{60}Fe_{37}Cu_3$single crystals in which an external magnetic field of 1.3 T was applied along different crystalline directions [2]. In the spectra analysis, hyperfine fields were modelled by a binomial distribution (resulting from assumed random arrangements of atoms in the *fcc* lattice). The experiment was sensitive enough to detect the dependence of the orientation of hyperfine field on the applied external field. However, within the binomial approximation used in [2], the observed anisotropy could not be fully explained.

To check whether the distribution of atoms in Fe–Mn alloy is really random, we performed experiments in which crystal was plastically deformed. One expects that plastic deformation induces a change of the short range order, which should result in a change of the distribution of hyperfine fields. The spatial arrangement of spins in plastically deformed crystal was investigated with the use of circularly polarized radiation in Mössbauer measurements. This technique is sensitive to the sign of the hyperfine field, e.g. it can distinguish between parallel and antiparallel orientation of the magnetic moments with respect to the photon **k** vector.

2. Experimental

A single crystal γ-$Mn_{60}Fe_{37}Cu_3$ alloy was grown by the Bridgman method. Small amount of Cu was added to stabilize the *fcc* structure. Three flat samples of the thickness of about 0.5 mm were cut with their surfaces parallel to (100), (110) and (111) crystal planes, respectively. The samples were thinned by grinding to about 50–60 μm. In the next step, the samples were thinned by electrochemical methods to the thickness suitable for the Mössbauer transmission experiment [2]. Part of the crystal with linear dimensions 0.9 mm was cold rolled to a foil 6 μm thick.

Mössbauer measurements were performed in constant acceleration mode with unpolarized radiation. When no external field is applied to the absorber, the shape of the Mössbauer spectrum does not depend on the orientation of the **k** vector with respect to the crystalline direction [2], and the spectrum averaged over all measurements is shown in Fig. 1a. For the measurements in the magnetic field, the samples were placed in the hole of the permanent rare earth magnet producing an axial field of 1.3 T. The field was parallel to the **k** vector of the radiation and perpendicular to the sample surface. An example of the spectrum for **k** and $\mathbf{B}_{ext}$ perpendicular to the (100) and (111) planes is shown in Figs. 1b, c. The difference spectrum is shown in Fig. 2.

Measurement on the plastically deformed foil was performed in a texture free mode [3] with unpolarized radiation. The result is shown in Fig. 3a and is equivalent to the measurements averaged over random orientations of the absorber. Results of the Mössbauer polarimetric measurements with the use of circularly polarized radiation obtained by resonant filter technique [4], carried out on the deformed crystals in an

external field of 1.1 T, are shown in Figs. 3b, c. All Mössbauer measurements were performed at room temperature.

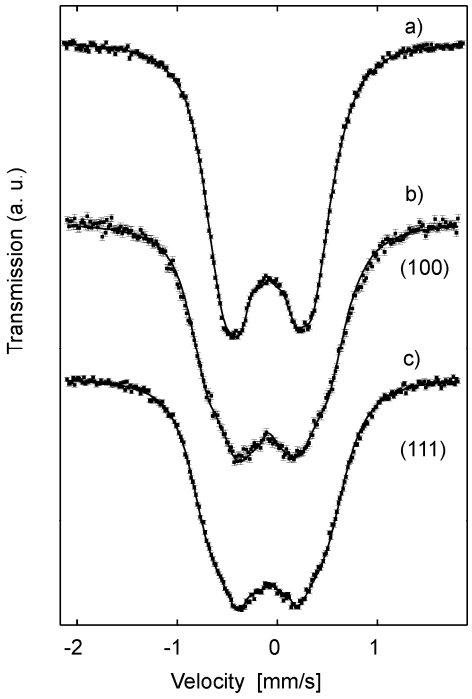

Fig. 1. Mössbauer spectra of a single crystal recorded with no applied external field (a), with external field of 1.3 T perpendicular to the (100) (b) and (111) (c) crystal planes

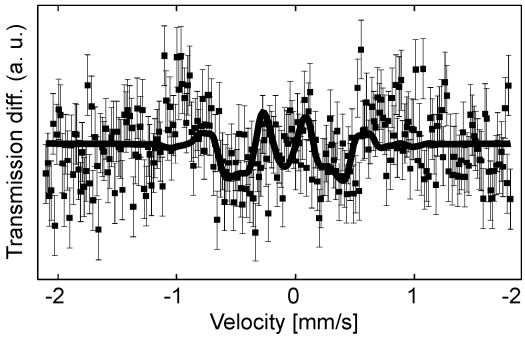

Fig. 2. Difference between the data shown in Fig 1b and c ((111) – (100)). The solid line shows the result of the simulation when Q_2 and Q_3 structures are present in the proportion 3:1

The principles of the Mössbauer polarimetric methods in the presence of a distribution of hyperfine fields are given elsewhere [5, 6]. We assume that the local hyperfine magnetic field $\mathbf{B}_{hf}$ is antiparallel to the Fe magnetic moments in the Q_i (i = 1, 2, 3) structure. The observed local field is a vector sum of the external magnetic field $\mathbf{B}_{\text{ext}}$ and the local hyperfine field $\mathbf{B}_{hf}$. Line intensities a_i in the Zeeman sextet are proportional to

$$\begin{aligned} a_1 : a_2 : a_3 : a_4 : a_5 : a_6 &= 3\left(1 \mp \cos\theta\right)^2 : 4\sin^2\theta : \left(1 \pm \cos\theta\right)^2 \\ &: \left(1 \mp \cos\theta\right)^2 : 4\sin^2\theta : 3\left(1 \pm \cos\theta\right)^2 \end{aligned} \tag{1}$$

where θ is an angle between the hyperfine magnetic field $\mathbf{B}_{ext} + \mathbf{B}_{hf}$ and the photon wave vector $\mathbf{k}$.

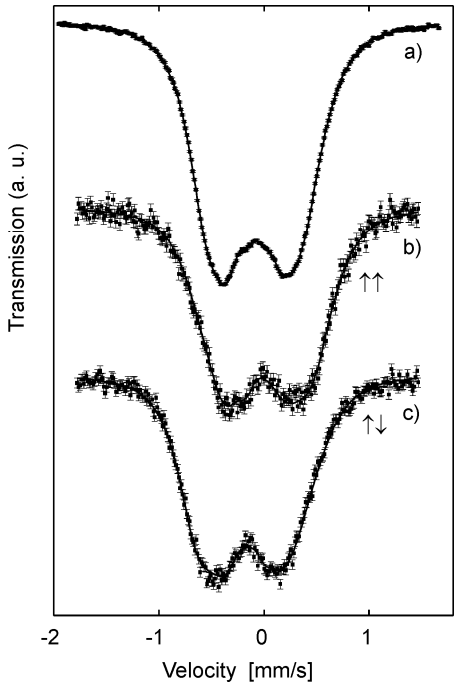

Fig. 3. Plastically deformed single crystal measured with: a) unpolarized radiation, b), c) circularly polarized radiation under an applied axial external magnetic field of 1.1 T. The arrows indicate two circular polarization states of the radiation. The solid lines, which show the best fits, are almost covered by the experimental points

Upper and lower signs correspond to the two opposite circular polarizations. In the case of unpolarized radiation, the expression is reduced to:

$$a_1 : a_2 : a_3 : a_4 : a_5 : a_6 = 3\left(1+\cos^2\theta\right) : 4\sin^2\theta : \left(1+\cos^2\theta\right) : \left(1+\cos^2\theta\right) : 4\sin^2\theta : 3\left(1+\cos^2\theta\right), \tag{2}$$

Next, we assume a certain distribution of the hyperfine magnetic field $P(|\mathbf{B}_{hf}|)$ and perform a simultaneous fit to all the spectra measured on single crystals. $P(|\mathbf{B}_{hf}|)$ distribution was approximated by the discrete set of $|\mathbf{B}_{hf,\mathbf{i}}|$ values and probabilities P_i. A nonlinear correlation between *IS* and $|\mathbf{B}_{hf}|$ was allowed, see Fig. 4. Zero quadrupole splitting was assumed according to previous investigations [1, 2]. Similar fit was performed to all the spectra measured on the deformed sample.

3. Results

For a given Q_i structure, the simultaneous fit procedure ("Mathematica" package used, for details of simultaneous fit and thickness correction see [5]) allows us to find $P(|\mathbf{B}_{hf}|)$ distribution for which agreement between measured and simulated spectra was

the best. We have found that for Q_1 structure, the agreement was definitely worse than for Q_2 and Q_3 structures. It was difficult to decide which of the two structures fits better. Moreover, we found that the best agreement is attained when the presence of both structures, Q_2 and Q_3 is assumed. This case is illustrated with typical examples in Fig 1, where ratio of volumes of the Q_2 and Q_3 phases was 3:1. To show clearly the anisotropy induced by an external field applied to a single crystal, difference of the spectra together with the difference of simulated curves are presented in Fig. 2. Some slight systematic deviation can be observed on the difference (Fig. 2), the origin of this behaviour being obscure. Nevertheless, the overall agreement shown in Fig. 1 is much better than in the already reported works [1, 2]. The distribution $P(|\mathbf{B}_{hf}|)$ found in the simultaneous fit to all measured spectra of single crystals is shown in Fig. 4 (note the areas of the circles).

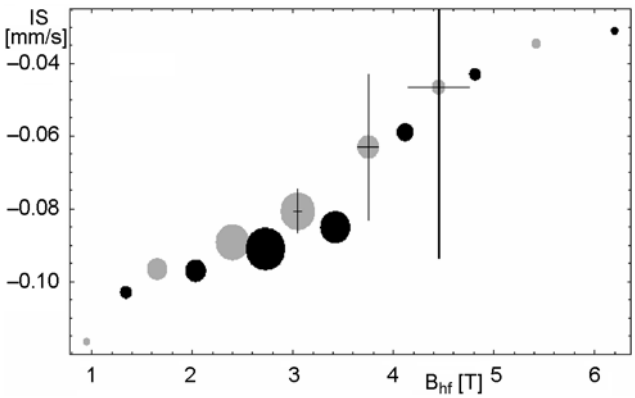

Fig. 4. Correlation between hyperfine magnetic field B_{hf} and isomer shift *IS*. The black circles correspond to single crystals, gray ones – to the plastically deformed samples. The area of the circle is proportional to the probability $P(|\mathbf{B}_{hf}|)$ and $P(IS)$

The plastically deformed sample is no longer a single crystal and was measured in the texture free mode in order to extract its distribution of the hyperfine field. As described in the previous section, all the experiments performed on the plastically deformed sample were simultaneously fitted under the assumption that the local field is equal to $\mathbf{B}_{\text{ext}}+\mathbf{B}_{hf}$, where and $\mathbf{B}_{hf}$ are arranged in random directions. The extracted hyperfine field distribution is shown in Fig. 4 by gray symbols and typical examples of the simulated spectra are shown in Fig. 3 by solid lines.

4. Discussion

In the interpretation of the results of the pioneering experiment of Kennedy and Hicks [1], the authors considered the movement of the domain walls. However, although the occupation of the domains was a free parameter, the shape of the simulated

spectra did not agree with the measured ones [1]. The presented results demonstrate clearly that the most important factor deciding on the agreement of simulated spectra with the measured ones is the shape of the distribution of hyperfine fields. A proper choice of the $P(|\mathbf{B}_{hf}|)$ function, achieved by fitting, results in the overall agreement of the measured spectra in zero field and in an applied external field. The method of determination of the $P(|\mathbf{B}_{hf}|)$ is so precise that it is possible to detect changes in short range order induced by plastic deformation. The differences, shown schematically in Fig. 4, can be presented clearly on the histograms (Fig. 5). It is clear from Fig. 5 that in the case of single crystals, both $P(|\mathbf{B}_{hf}|)$ and $P(IS)$ distributions, are narrower. Plastic deformation causes a slip of atomic planes resulting in the mixing of atoms and a more random distribution.

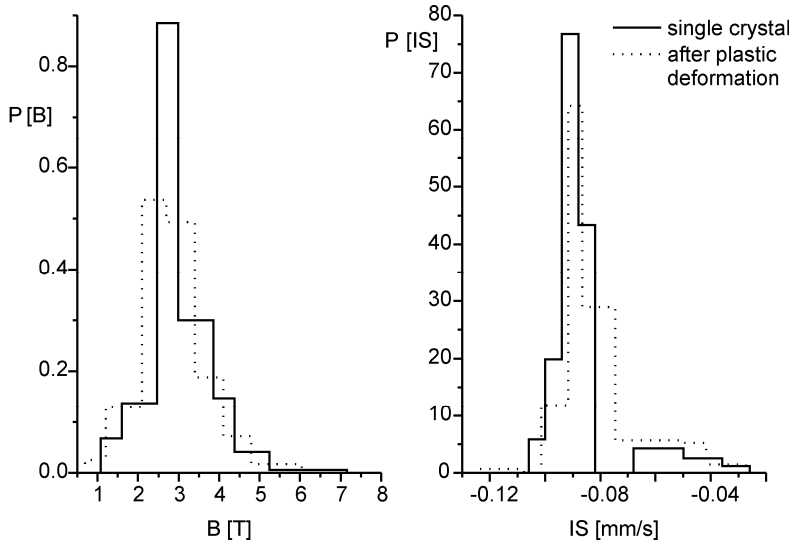

Fig. 5. Histograms related to $P(|\mathbf{B}_{hf}|)$ and $P(IS)$ distributions

The measurements with polarized radiation show that the spatial arrangement of magnetic moments remains unchanged, i.e. the recorded spectra can be explained by rigid arrangements of local hyperfine field vectors plus the external applied field. This picture is consistent with recent self-consistent tight binding linearized muffin-tin orbital approach allowing a noncollinear spin structure. It was shown that the ground spin states in a fully ordered and fully disordered gamma Fe–Mn alloys are different and their spin ordering is driven by the random substitutional disorder, a phenomenon known as ordering due to disorder [7]. In the measurements with circularly polarized radiation, only the Fe system is detected as a nuclear ^{57}Fe probe. Thus, the presented results show that in the system under investigation we do not observe, within an experimental accuracy, an antiparallel ordering of two systems: Fe and Mn. This important point was considered in electronic band structure calculations [8].

As presented in the previous section, the assumption regarding the presence of Q_2 or Q_3 state in a single crystal leads to a similar quality of the simultaneous fit, while the best agreement of simulations and measurements being obtained when the presence of both structures was assumed. This observation is in agreement with the first principles electronic structure calculations of noncollinear magnetic structures [8]. The Korringa–Kohn–Rostocker multiple-scattering approach, in conjunction with an extension of the single site coherent potential approximation, show that the Q_3 and Q_2 structures are both stable solutions. The energy difference between the two noncollinear states is relatively small with the Q_3 being more favorable. It was mentioned [8] that the difference, which corresponds to 60 K, is so small that the systems may occupy both states.

5. Conclusions

We have shown that in order to understand the magnetism of the alloy under study, a precise determination of the shape of the hyperfine magnetic field (h.m.f) distribution is required. Plastic deformation changes the short range order of atoms in a measurable way resulting in a change of the h.m.f. distribution. Among the two possible reasons influencing the shape of the spectra under the applied external field, i.e. the movement of domain walls and the presence of h.m.f. distribution, the latter one is more important.

Adjusting properly the shape of the distribution, we performed fits which indicate that Q_1 structure cannot be accepted, Q_2 and Q_3 structures result in a similar quality of the fits, while the assumption regarding the presence of both Q_2 and Q_3 structures gives the best fits. This can be expected from the results of the theoretical band structure calculations which indicate a small energy difference between Q_2 and Q_3.

References

[1] KENNEDY S.J., HICKS T.J., J. Phys. F: Met. Phys., 17 (1987), 1599.
[2] SZYMANSKI K., OLSZEWSKI W., DOBRZYNSKI L., SATULA D., JANKOWSKA-KISIELINSKA J., Nukleonika, 49 (2004), S75.
[3] GRENECHE M.J., VARRET F., J. Phys.-Lett., 43 (1982), L-233.
[4] SZYMAŃSKI K., DOBRZYŃSKI L., PRUS B., COOPER M.J., Nucl. Instr. Meth., B119 (1996), 438.
[5] SZYMANSKI K., SATULA D., DOBRZYNSKI L., VORONINA E.V., YELSUKOV E.P., MIYANAGA T., Phys. Rev. B 72 (2005), 104409.
[6] SZYMANSKI K., Phys. Rep. 423 (2006), 295.
[7] SPISAK D., HAFNER J., Phys. Rev. B, 61(2000), 11569.
[8] SCHULTHESS T.C., BUTLER W.H., MAAT S., MANKEY G.J., STOCKS G.M., J. Appl. Phys. 85(1999), 4842.

Received 7 May 2006
Revised 1 September 2006